Hindawi Publishing Corporation
International Journal of Distributed Sensor Networks
Volume 2012, Article ID 865184, 9 pages
doi:10.1155/2012/865184

Research Article

Improving Accuracy for 3D RFID Localization

Jinsong Han,[1] Yiyang Zhao,[2] Yan Shun Cheng,[3] Tse Lung Wong,[3] and Chun Hung Wong[3]

[1] *School of Electronic and Information Engineering, Xi'an Jiaotong University, Xi'an 710049, China*
[2] *School of Software, TNLIST, Tsinghua University, Beijing 100084, China*
[3] *Department of Computer Science and Engineering, HKUST, Kowloon, Hong Kong*

Correspondence should be addressed to Jinsong Han, hanjinsong@mail.xjtu.edu.cn

Received 15 December 2011; Accepted 4 February 2012

Academic Editor: Mo Li

Radio Frequency Identification (RFID) becomes a prevalent labeling and localizing technique in the recent years. Deploying indoor RFID localization systems facilitates many applications. Previous approaches, however, are most based on 2D design and cannot provide 3D location information. The lack of one-dimensional information may lead 2D-based systems to inaccurate localization. In this paper, we develop an indoor 3D RFID localization system based on active tag array. In particular, we employ the geometric mean to filter the explicit 3D location information with high accuracy. The experimental results show that our system is efficient in tracking objects and improving the localization accuracy.

1. Introduction

As a more efficient way of identifying objects than conventional Barcode technique, Radio Frequency Identification (RFID) technology has been popular in many applications, such as surveillance, access control, theft prevention, and movement tracking [1–4]. An RFID system comprises of a number of readers and a large amount of tags. The tag usually stores an ID that is uniquely assigned. When entering or staying in the interrogation area of readers, a tag can report its ID to the reader via RF signals. The reader can retrieve the data sent from the tag with predefined radio frequency and protocols. In practice, the frequency ranges between 135 KHz, 13.56 MHz, UHF (433 MHZ, for active tags, 860 to 960 MHz for passive tags), and 2.45 GHz. There are two main types of tags, passive tags and active tags. Passive tags absorb energy from the RF wave emitted from the reader and hence do not have onboard energy supply. On the contrast, active tags are equipped with onboard power supply, usually using button-cell batteries, so that they can actively operate in a longer communication range than passive tags. The RFID technology offers very attractive advantages. For example, using RFID can achieve a noncontacting and non-line-of-sight processing pattern, which allows the system to automatically collect the data from items with which the tags are attached or embedded.

The RFID can play many important roles in existing applications. In this paper, we are interested in using active RFID tags for 3D localization. Traditionally, if we plan to monitor a large area, an intuitive solution is to deploy many cameras for surveillance. However, the visual-based monitoring system suffers from several drawbacks. A camera could only monitor in a fixed direction. If we are aiming at a full coverage of monitoring over a large region, many cameras may be deployed, which renders high cost. Meanwhile, the detection of objects' complete trajectories is difficult within large areas. Deploying video systems may cause some gaps or holes in the coverage of surveillance, which will produce discontinuous trajectory reporting. Last but not least, the objects' trajectories should be predefined if using video systems. Detecting nonregular or unpredicted moving objects is thereby nontrivial.

As utilizing the RSSI in wireless networks for localization [5, 6], the strength (and its changes) of RF signals could be utilized to locate and hence track objects. On the other hand, the readers and tags emit their RF signal in an omni-directional way, which closes the gap of monitoring coverage. In addition, the deployment pattern of RFID systems is more flexible than that of video-based systems. Redeployment may be not necessary even if the object moves very abnormally or unpredictably.

Many efforts have been made for locating objects based on RSSI or RF signals [2, 3, 7–11]. Most of them, however, focus on two-dimensional (2D) scenarios. In practice, however, many applications are deployed in 3D terrains, such as an inventory management system deployed in a warehouse with many shelves, a structural monitoring network mounted on an aged building, or a surveillance system implemented in a theater or gym, and so forth. Missing any coordinate in the 3D space would seriously constrain the accuracy or completeness of localization.

In this paper, we propose to break above limitation and extend the 2D localization to 3D scenarios. We implement RF-based 3D localization system with active RFID tag array based on a classical 2D localization work, VIRE [7]. VIRE utilizes reference tags for locating a target tag. Although the VIRE algorithm eliminates unlikely positions, it is still computationally inefficient, especially when being extended to 3D implementation. Our approach adopts a simple mechanism, geometric mean, to improve the efficiency of eliminating unlike positions of tracking tags, which also improves the efficiency of 3D localization when using the RF reference tags. The experimental result demonstrates the effectiveness and efficiency of our system.

The rest of the paper is organized as follows. Section 2 briefly discusses the related works. We present our design in Section 3 and implementation in Section 4. We evaluate the performance of our system in Section 5 and conclude in Section 6.

2. Related Work

As a promising wireless identification technology, RFID has been increasingly important in both the research and industry communities [2, 3, 12–15]. The research issues of RFID study in the literature focus on the anticollision, security, and localization.

Collisions significantly lag the identification speed in RFID systems. There are two types of signal collisions: *tag collision*, which may occur when more than one tag responds simultaneously; *reader collision*, which will happen when a region is overlapped by two or more readers' scanning signals. Anti-tag-collision approaches are divided into two categories, Framed-Slotted-ALOHA- (FSA-) based and Binary-Tree- (BT-) based algorithms. Roberts [16] first proposes an FSA-based anticollision scheme. Later, Lee et al. [17] claims that a maximum identification throughput can be achieved when the size of frame equals the number of tags. EPC Gen2 [18], a widely deployed RFID standard, adopts "Q-Adaptive" to adaptively adjust the frame length according to previous slots. Another well-known RFID air protocol, ISO 18000-6 [19], employs the Binary-Tree- (BT-) based RFID identification protocol. Hush and Wood [20] analyze the throughput of BT-based algorithms in [21]. Myung and Lee [22] then propose an adaptive binary splitting (ABS) protocol to reduce collisions. Besides tag collisions, reader collision is also challenging in large-scale RFID deployments. Existing solutions focus on assigning different channels to adjacent readers [23] or scheduling their interrogations into different rounds [24].

Meanwhile, some approaches [25, 26] have been proposed to achieve authentication in RFID applications. To prevent tags from being tracked, Weis et al. propose a hash-function-based authentication scheme, Hash Lock [27]. Hash Lock, however, has a slow authentication speed due to its $O(N)$ key search complexity, where the N is the total number of tags in the system. Some subsequent attempts aim at reducing the cost of key search. Different from the linear key organization, tree-based structures can reduce the search complexity from $O(N)$ to $O(\log N)$ [25]. Choi and Roh propose such a scheme [26]. Lim et al. [28] presents a randomized-bit-encoding scheme to enhance the security protection for RFID tags. The RFID privacy models have been extensively studied in [29].

The employment of radio signal strengths for indoor localization is very popular. Besides the identification, RFID tags can also facilitate the localization by using their RF signals. For the RFID-based localization, LANDMARC is one of the pioneering works. LANDMARC [2] introduces the reference tags and predefines the location map of reference tags to facilitate tracking tags. In LANDMARC, four reference tags that are nearest to the tag attached to the targeted object. The RSSI reported from those tags will be compared to predefined map and hence to approximate the location of the tag tracked. Later, VIRE [7] is proposed as an advance method based on LANDMARC. In VIRE, four reference tags form a grid, and some reference tags will be interpolated in the grid. Then a proximity map is obtained after collecting the results by the RFID readers. The algorithm of VIRE estimates and filters unlikely positions by intersection. Compared with LANDMARC, VIRE is more accurate but with more computational overhead. To our knowledge, there are little efforts focusing on the 3D RFID localization. Utilizing resource-limited wireless devices, for example, the RFID tag, for 3D localization is still difficult.

3. 3D RFID Localization Design

In this section, we present the design of our system. Our system works in following steps: (1) system deployment, (2) RSSI data collection and analysis, (3) tracking targeted tags, and (4) refining the location of targets. First, we establish the tag array in the deploying region. We then collect the strength of RF signals in the initialized system. After an extensive analysis, the strength distribution of RF signals can be retrieved. We design an efficient algorithm for 3D localization based on the signal strength to track targeted tags. Last, we refine the location regions for targets by using a simple but effective condensation process, the geometric mean calculation.

3.1. System Deployment. We employ the active tags, M100, manufactured by RF Code [30], to implement a prototype framework. The active tags work on the 433 MHz and have a transmission range up to 300 feet. Figure 1 shows the deployment of RFID readers and tags in the tag array system.

We deploy a 3D array of RF tags in the monitoring field. The active tag will broadcast a probing message, including its unique ID and status information at each time unit (we term

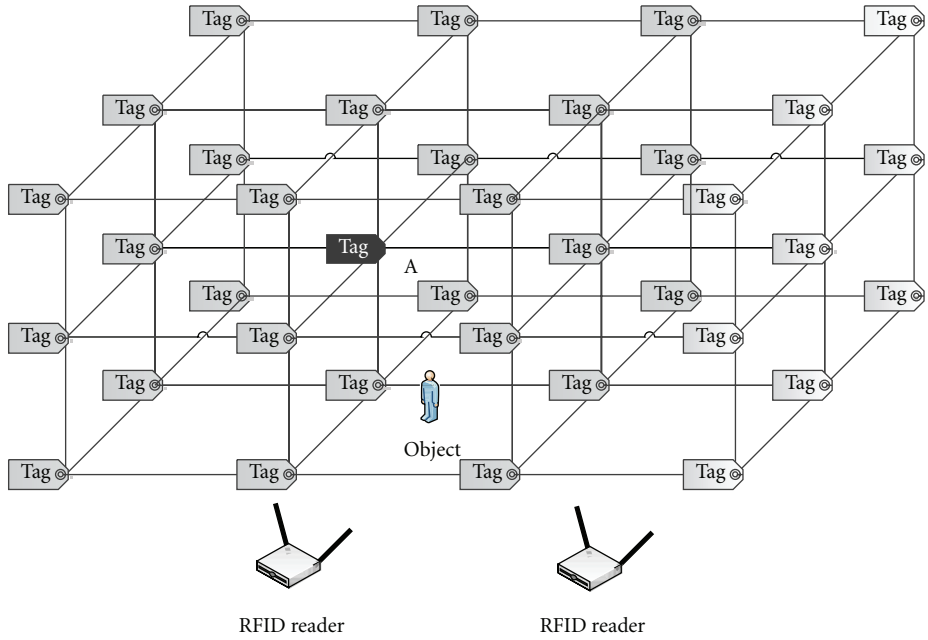

Figure 1: Tag array deployment.

such a unit as *period* in this paper). The beacon rates for these tags range from 2 seconds to 10 seconds, based on the user specification or application requirements. There is no synchronization mechanism among the tags. All the tags compete for the transmission window.

Besides the tags, we also deploy a small number of readers (in our preliminary system, the number is 2) for collecting the signals emitted from tags. Note we do not need to deploy too many readers because the reading range of readers is relatively large. The reader can cover a distance of more than 1,000 feet. In practice, the reading range depends on the antenna configuration. The readers are connected to a server within a LAN. In our system, the reader can collect the essential information about tags, including the tag ID, the reader ID, and RSSI.

3.2. RSSI Data Collection and Analysis. Before performing the localization, the system first reads tags' RSSI from the reader and store in database together with their physical location coordinates. The gathered tags' RSSI values together with the pre-defined reference tags' coordinates, as shown in Figure 2, are stored into our database for later localization and further analysis.

However, the RSSI values collected by the reader are raw and messy. Some of them fluctuate a lot. We filter the raw data to make it more accurate and useful. There are two antennas in each reader. The reader will report that two RSSI values for each tag correspond to the two antennas. Sometimes the signal cannot be detected due to the interference. We adopt the following policy to maintain a good estimation of the RSSI. If both antennas report values, we take the average. If only one of the antennas provides a value, we take it as the resultant value. If both antennas do not provide a value, we take a value of −1 to label that tag as not-detected, as shown in Figure 3. The smaller the RSSI value is, the longer of the distance between the tag and the readers.

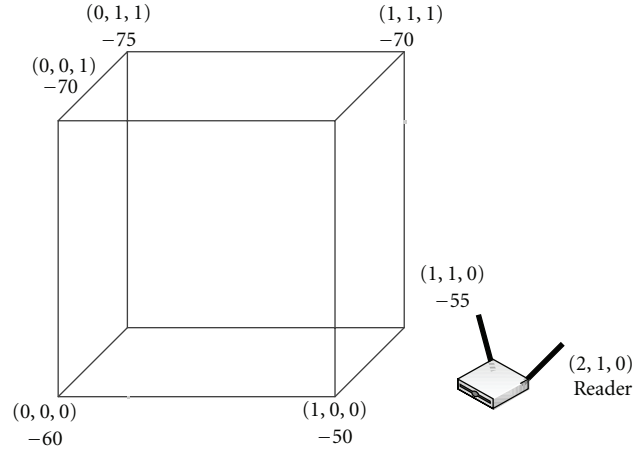

Figure 2: Reference tags' RSSI and predefined coordinates.

3.3. Virtual Reference Tag. We adopt the basic algorithm of VIRE [3] to calculate the virtual tags' RSSI and location to find out tracking tags' location. The VIRE algorithm works as follows.

It can be observed that if other environment factors keep unchanged, the active tag placed in the same position will present similar RSSI [7]. Therefore, one tag's RSSI can be estimated if its position is sufficiently close to a tag whose position is already known. To leverage this phenomenon,

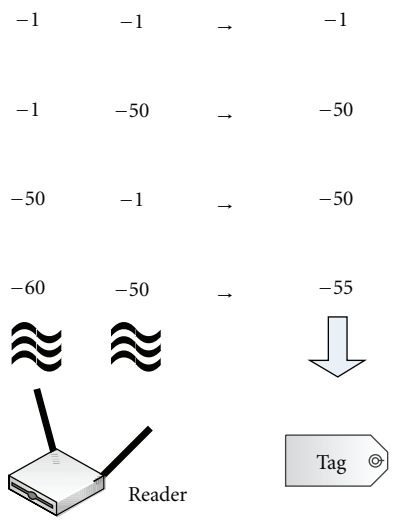

Figure 3: Determining RSSI for each tag.

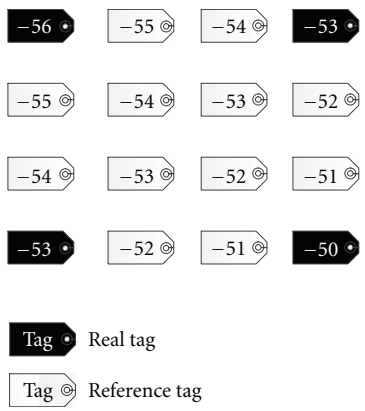

Figure 4: Interpolation of virtual reference tags' RSSI.

LANDMARC and VIRE use the reference tags to track other tags in the deploying area.

In common scenarios, the deployment of reference tags is sparse due to the cost consideration. In order to increase the accuracy, VIRE introduces virtual reference tags without increasing the number of real readers or tags, as shown in Figure 4. The RSSI values and coordinates of virtual reference tags are then calculated based on the real tags. In our approach, we also introduce virtual reference tags. We adopt the major principle of VIRE and then extend it from 2D to 3D, as illustrated in Figure 5.

The determination method of reference tags' RSSI is similar to VIRE, which is calculated by using the linear interpolation algorithm. According to VIRE, $n-1$ virtual reference tags should be equally placed between two adjacent real tags. After performing the linear interpolation algorithm, the RSSIs of virtual tags at both the vertical and horizontal directions can be computed. As shown in Figure 4, if we insert $n-2$ tags between two adjacent real tags, a $n \times n$ tag array can be obtained. To interpolate the RSSI of virtual tags in the 3D deployment, we first perform the VIRE algorithm on the upper and lower planes while treating them as two separate 2D cases. With the results on these two planes, we can easily extend the process to 3D. Finally, we can generate a 3D RSSI distribution of all tags in the deploying area.

3.4. Tracking Targeted Tags. After the 3D virtual reference distribution is retrieved, the RSSI value of each virtual reference tag can be used to track targeted tags. We can measure the RSSI value of the targeted tag via each reader. We then seek the matching between the tracked tag and some reference tags. In our approach, we select the reference tag(s) by using a threshold. The threshold is defined as the maximum acceptable difference between the targeted tags and reference tags. Thus, the positions of those reference tags with a difference smaller than the threshold from the targeted tag are potential locations of the tracked tags. In practice, many positions may be selected as the potential locations given an RSSI value of targeted tag. We employ the proximity map [7] to reflect the possible locations of tracked tags, while our approach extends the map to a 3D grid. Once the reference tags that are located at the potential locations of targeted tag are selected, the reader marks those regions as "1" in its proximity map. In practice, each reader will maintain such a map.

Intuitively, we integrated the proximity maps from the readers deployed in the detecting area. An intersection function is performed and then we filter the most probable regions of target from all readers. The so-called elimination will remove the unlikely positions. Here, determining a proper threshold is very important. The detail setting of threshold and the algorithm of elimination can refer to VIRE [7].

3.5. Refining the Location of Target. However, simply intersecting the proximity maps may be also inaccurate in terms of the scope of potential regions outlined by VIRE. We further improve the localization accuracy by "shrinking" the regions of potential positions. We employ two methods to achieve the refinement. First, we convert the raw 3D proximity maps into a 3D density map. Second, we compute the geometric mean of potential location and its surrounding locations in the 3D density map.

We employ a 3D array to contain the 3D proximity map. It included both the reference tags' locations and virtual tags locations. The array first stores "True" or "False" of the location to log whether the tracked tag is present. In most cases, the "True" location is not unique, as illustrated in Figure 6(a). In this example, we show a $3 \times 3 \times 3$ 3D reference tag array.

The 3D density map can be derived from 3D proximity map. The 3D density map stores the number of "True" locations surrounding one of locations in the 3D proximity map. Note that a location has 26 adjacent locations if this location is fully surrounded by its neighboring locations. For example, in Figure 1, the location of A where the tag is in black color has 26 adjacent locations and its reference tags are in gray color. Our objective is to find out the most densely region of "True" locations. For a given location, if one of

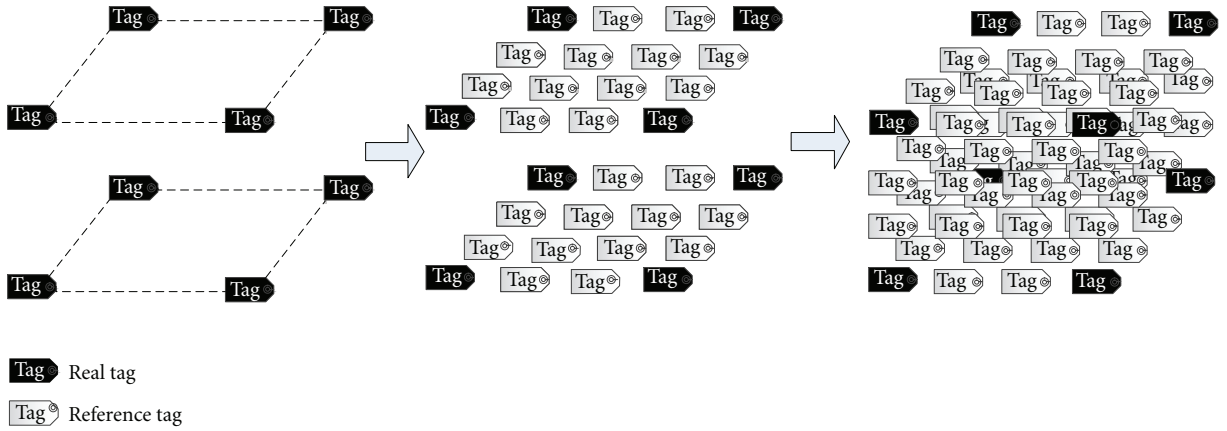

Figure 5: 3D virtual reference tag generation.

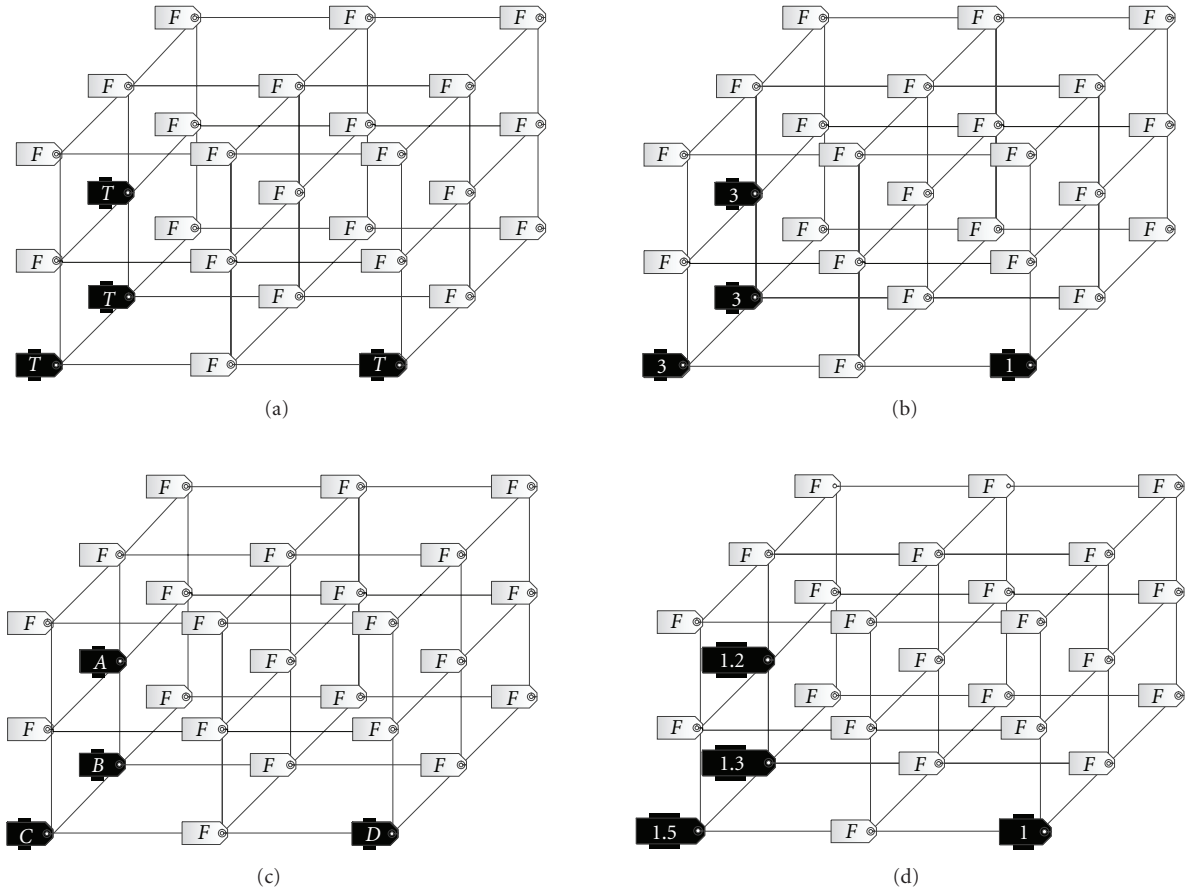

Figure 6: One of levels of a $3 \times 3 \times 3$ 3D proximity map.

its adjacent locations in the 3D proximity map is "False," no value will be added to this location. Otherwise, if the value is "True," its value will be added by 1. For the example in Figure 6, Figure 6(b) is the 3D density map converted from the 3D proximity map of Figure 6(a). In Figure 6(c), we represent the locations with "True" values in Figure 6(a) as location A, B, C, and D, respectively. After the counting process, the values of locations become 3, 3, 3, and 1.

In case that the setting of threshold value is large, the dense region may not be unique in the 3D density map. In order to reduce the region and achieve more accurate location, we conduct a condensation process in the 3D

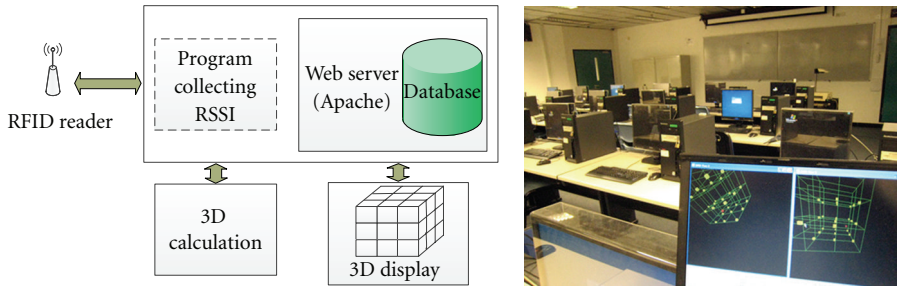

(a) (b)

Figure 7: The components of our system and implementation in the indoor environment.

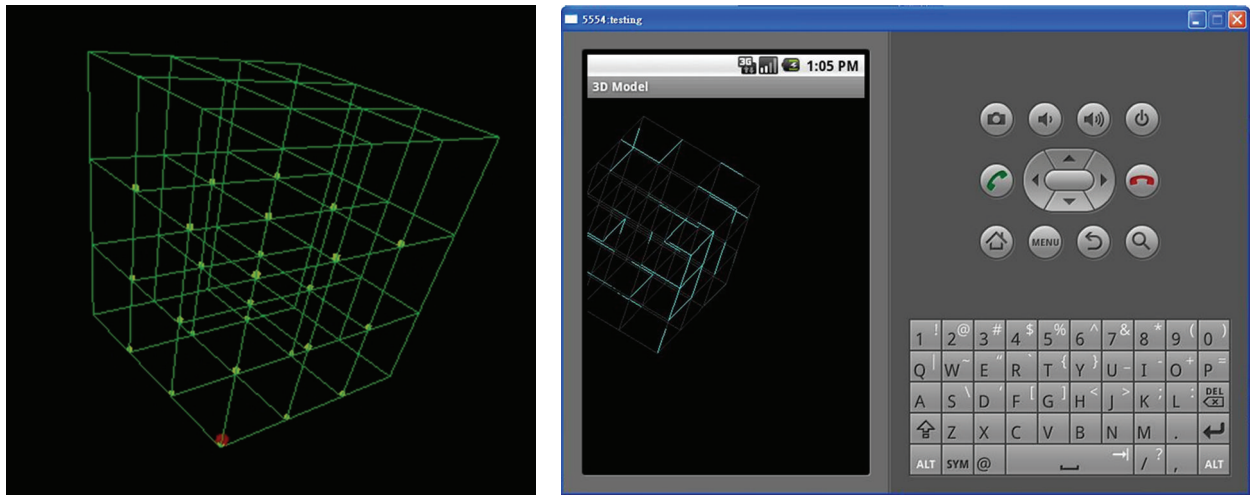

(a) (b)

Figure 8: 3D effect in GUI and the simulated operating interface in mobile phone.

density map. The principle of this process is to drive the edge locations which have smaller values of density to be closer to the higher density part. We calculate the geometric mean among the given location and its adjacent locations. This process will be continued if the dense region of locations is not unique, until a unique highest density location occurs.

For example, in Figure 6(d), the calculation of four black tags' locations is as follows:

$$A = \sqrt[18]{3^3} \approx 1.2, \quad B = \sqrt[12]{3^3} \approx 1.3, \quad c = \sqrt[8]{3^3} \approx 1.5, \quad D = \sqrt[8]{1} = 1. \tag{1}$$

4. Implementation

We deploy the tags and readers in an indoor environment. The distance between two adjacent tags is one meter. The readers are placed in the corners of the sensing area. The location of reference tags and readers are represented in a 3D coordinate system. The beacon interval is 2 seconds.

We develop a 3D model program to display the location of tags on a graphical interface. This GUI can provide the user with both the overlook and detailed information about targeted tags' locations. We show the system deployment in Figure 7 and the prototype GUI of mobile phone in Figure 8.

We use Java to construct the 3D display model. It can be displayed on the mobile phone which supports the Java application. Our 3D model consists of an animation of 30 frames per second and it will continue to update the tag's coordinates of its location.

In the experiment, we mainly focus on examining the accuracy of the tracking tags. To simulate the practical application scenarios, we placed our setting in an empty classroom. Due to the limitation of the small size of the classroom, the setting was scaled down. The reference tags were placed in a $3\times3\times3$ 3D grid. Based on this grid, we set up a 3-dimensional coordinate system in the deploying room. The reference tags are placed on the floor, chairs, and tables for different levels. The values of z-coordinate of tags placed on the floor, chair, and table are 0, 1, and 2, respectively. The readers are placed at a coordinate of (0, 0, 2) and (1, 0, 2). We introduce 3 targeted tags placed at the position of (0.5, 1.5, 2). We connected 2 readers with LAN.

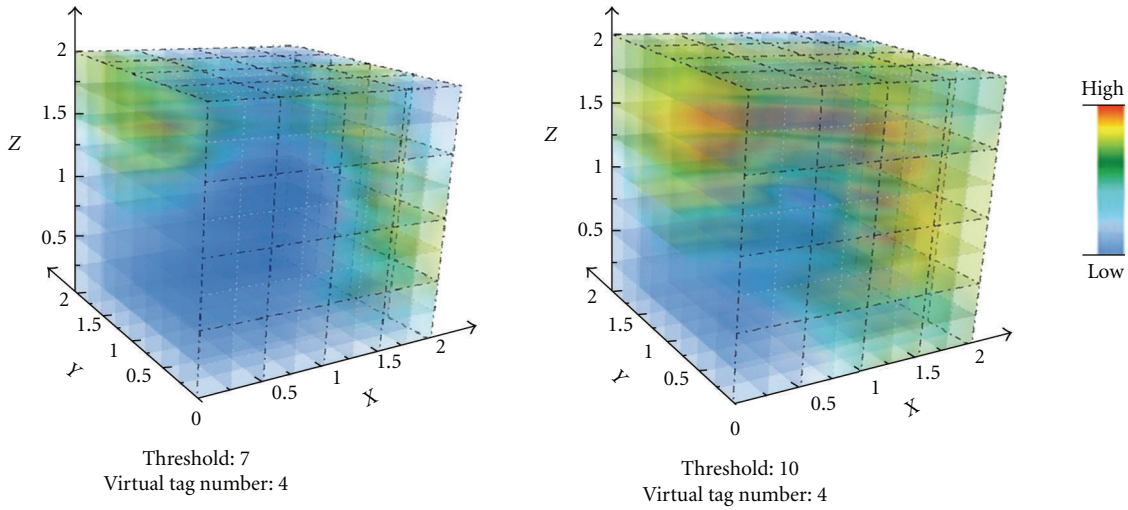

Threshold: 7
Virtual tag number: 4

Threshold: 10
Virtual tag number: 4

Figure 9: Performance under different threshold values.

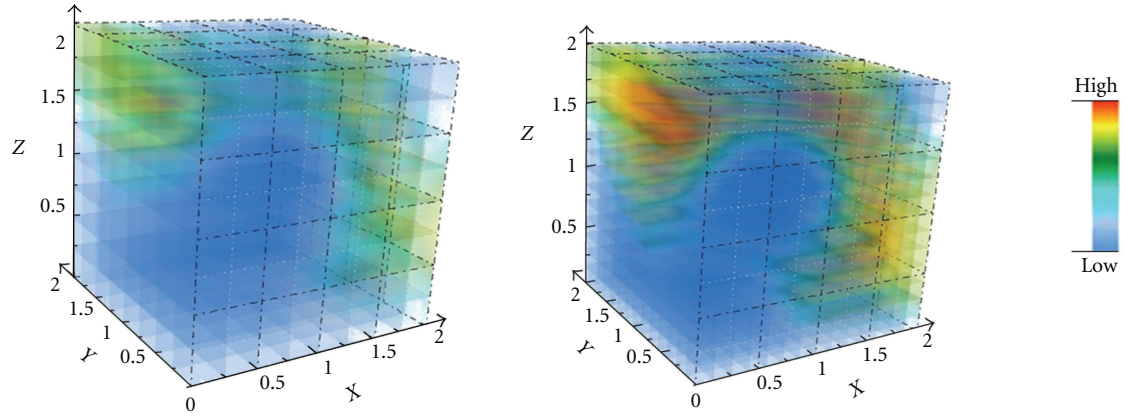

Threshold: 7
Virtual tag number: 4

Threshold: 7
Virtual tag number: 7

Figure 10: Performance with different numbers of virtual tags.

5. Evaluations

We examine the performance of localization with two matrixes. We first evaluate the impact of threshold settings. We then study the performance with different numbers of tags inserted into the 3D grid. We also check the diversity effect of tags. We finally investigate the localization errors of our approach.

5.1. Threshold Value. Figure 9 shows the effects on the density map with different threshold values 7 and 10. We can observe that the location of (0.5, 1.5, 2) is with the highest density value and with a very small region as the reported target location. In the contrast, the distribution of possible locations of target tag becomes much larger if the threshold is set as10 than the setting of 7. This indicates that the higher the threshold value is, the higher the error will be. Therefore, it is appropriate to set a small threshold value. In our experiments, the RSSI value changes around 5 units. We then set the threshold value as 5~7. In practice, we suggest that the optimal threshold value can be set according to user specification or the sensitivity of RFID devices.

5.2. Different Virtual Tag Numbers. We then examine the impact of the number of virtual tags and show the result in Figure 10, where the virtual tag numbers are 4 and 7 between two real tags. We can find that the resolution of target location becomes higher when changing the setting from 4 to 7. It can be concluded that setting a larger number of virtual tags tenders more accurate location report. As the number of virtual tags increases, the resulting location will be more precise. However, introducing more virtual tags would cause much more computational workload. In our experiments, we observe that setting the number of virtual tags from 4 to 7 yields acceptable workload to the server while keeping satisfied localization accuracy.

5.3. Comparison on Different Tracked Tags. We also check the performance change when tracking different tags. Figure 11

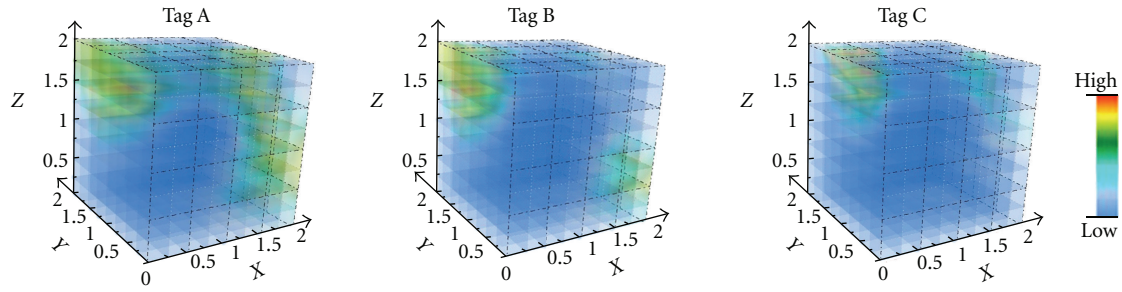

Figure 11: Comparison on different tracking tags.

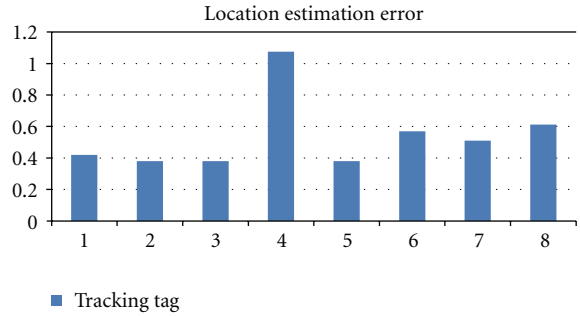

Figure 12: Estimation error.

plots the result of tracking three tags. We adopt the setting of 7 as the threshold and 4 as the number of virtual tags. We randomly select three tags, A, B, and C. We then place them in the same position. We observe that their density maps are similar. The reported possible location regions of three tags are almost same, while the calculated locations of three tags are very close to (0.5, 1.5, 2).

5.4. Location Estimation Error. The location estimation error is the distance between the real position of tracked tag and the computed position. Suppose the former is (x_0, y_0, z_0) and the latter is (x, y, z). To compute the estimation error e, we have the following formula:

$$e = \sqrt{(x - x_0)^2 + (y - y_0)^2 + (z - z_0)^2}. \quad (2)$$

In order to compute the location estimation errors, we still use the same testbed as above, but the locations of the tracked tags are at the center of the 4 reference tags. We show their coordinates in Table 1.

From the formula, the e of 8 tags is shown in Figure 12. The readers are placed at two positions (0, 0, 2) and (1, 0, 2). For Tag-1, Tag-2, and Tag-3 that are placed close to the readers, their estimation errors are around 0.4 m. For Tag-6, Tag-7, and Tag-8, which are placed far away from the readers, the estimation errors are about 0.55 m. In particular, the interference at Tag-4 is so strong that the error approaches 1.1 m at that position. From the result, we learn that the estimation error is higher when the distance between the readers and the tracking tag becomes larger. In addition, the average estimation error of 8 tags is 0.54 m. In the 3D grid, each reference tag is assumed to be placed with a 1-meter distance with its adjacent tags. To summarize, the accuracy of the system is acceptable for the indoor application.

Table 1: Coordinates of tracked tag.

Tracking tag	x	y	z
1	0.5	0.5	0.5
2	0.5	0.5	1.5
3	1.5	0.5	0.5
4	1.5	0.5	1.5
5	0.5	1.5	0.5
6	0.5	1.5	1.5
7	1.5	1.5	0.5
8	1.5	1.5	1.5

6. Conclusion

In this paper, we propose a 3D RFID localization technology. The work extends the RFID-based localization from 2D to 3D space and refines the location regions from pervious works. The experiment result shows the feasibility and effectiveness of our work. Our future work will focus on the implementation of proposed systems in more real RFID applications.

Acknowledgments

This work is partially supported by the National Key Basic Research and Development Program (973) of China

under Project no. 2011CB302705, NSFC under Project no. 61033015 and no. 60903155, and the Fundamental Research Funds for the Central Universities of China.

References

[1] C. Qian, H. Ngan, Y. Liu, and L. M. Ni, "Cardinality estimation for large-scale RFID systems," *IEEE Transactions on Parallel and Distributed Systems*, vol. 22, no. 9, pp. 1441–1454, 2011.

[2] M. N. Lionel, Y. Liu, Y. C. Lau, and A. P. Patil, "LANDMARC: indoor location sensing using active RFID," *Wireless Networks*, vol. 10, no. 6, pp. 701–710, 2004.

[3] Y. Liu, L. Chen, J. Pei, Q. Chen, and Y. Zhao, "Mining frequent trajectory patterns for activity monitoring using radio frequency tag arrays," in *Proceedings of the 5th Annual IEEE International Conference on Pervasive Computing and Communications (PerCom '07)*, pp. 37–46, March 2007.

[4] Y. Zheng, M. Li, and C. Qian, "PET: probabilistic estimating tree for large-scale RFID estimation," in *Proceedings of the International Conference on Distributed Computing Systems*, pp. 37–46, Minneapolis, Minn, USA, 2011.

[5] M. Li and Y. Liu, "Rendered path: range-free localization in anisotropic sensor networks with holes," *IEEE/ACM Transactions on Networking*, vol. 18, no. 1, Article ID 5280252, pp. 320–332, 2010.

[6] Z. Yang and Y. Liu, "Quality of trilateration: confidence-based iterative localization," *IEEE Transactions on Parallel and Distributed Systems*, vol. 21, no. 5, Article ID 5066966, pp. 631–640, 2010.

[7] Y. Zhao, Y. Liu, and L. M. Ni, "VIRE: active RFID-based localization using virtual reference elimination," in *Proceedings of the 36th International Conference on Parallel Processing in Xi'an (ICPP '07)*, September 2007.

[8] Y. Liu, Z. Yang, X. Wang, and L. Jian, "Location, localization, and localizability," *Journal of Computer Science and Technology*, vol. 25, no. 2, pp. 274–297, 2010.

[9] M. Li, W. Cheng, K. Liu, Y. Liu, X. Li, and X. Liao, "Sweep coverage with mobile sensors," *IEEE Transactions on Mobile Computing*, vol. 10, no. 11, pp. 1534–1545, 2011.

[10] X. Wu, S. Tan, T. Chen, X. Yi, and D. Dai, "Distributed dynamic navigation for sensor networks," *Tsinghua Science and Technology*, vol. 16, no. 6, pp. 648–656, 2011.

[11] L. Wang and W. Liu, "Navigability and reachability index for emergency navigation systems using wireless sensor networks," *Tsinghua Science and Technology*, vol. 16, no. 6, pp. 657–668, 2011.

[12] B. Sheng, C. C. Tan, Q. Li, and W. Mao, "Finding popular categories for RFID tags," in *Proceedings of the 9th ACM International Symposium on Mobile Ad Hoc Networking and Computing (MobiHoc '08)*, pp. 159–168, Hong Kong, May 2008.

[13] T. Kriplean, E. Welbourne, N. Khoussainova et al., "Physical access control for captured RFID data," *IEEE Pervasive Computing*, vol. 6, no. 4, pp. 48–55, 2007.

[14] C. Tan, B. Sheng, and Q. Li, "Efficient techniques for monitoring missing RFID tags," *IEEE Transactions on Wireless Communications*, vol. 9, no. 6, Article ID 5475333, pp. 1882–1889, 2010.

[15] D. Zhang, J. Zhou, M. Guo, J. Cao, and T. Li, "TASA: tag-free activity sensing using RFID tag arrays," *IEEE Transactions on Parallel and Distributed Systems*, vol. 22, no. 4, pp. 558–570, 2011.

[16] L. G. Roberts, "ALOHA packet system with and without slots and capture," *SIGCOMM Computer Communication Review*, vol. 5, no. 2, pp. 28–42, 1975.

[17] S. R. Lee, S. D. Joo, and C. W. Lee, "An enhanced dynamic framed slotted ALOHA algorithm for RFID tag identification," in *Proceedings of the 2nd Annual International Conference on Mobile and Ubiquitous Systems: Networking and Services (MobiQuitous '05)*, pp. 166–172, July 2005.

[18] EPCGlobal, "EPCGlobal radio-frequency identity protocols class-1 generation-2 UHF RFID protocol for communications at 860 MHz-960 MHz," Technical Report, 2005.

[19] ISO, "Information technology—radio frequency identification for item management—Part 6: parameters for air interface communications at 860 MHz to 960 MHz," Technical Report ISO Standard No. ISO/IEC 18000-6, 2004.

[20] D. R. Hush and C. Wood, "Analysis of tree algorithms for RFID arbitration," in *Proceedings of the IEEE International Symposium on Information Theory*, 1998.

[21] J. I. Capetanakis, "Tree algorithms for packet broadcast channels," *IEEE Transactions on Information Theory*, vol. 25, no. 5, pp. 505–515, 1979.

[22] J. Myung and W. Lee, "Adaptive binary splitting: a RFID tag collision arbitration protocol for tag identification," *Mobile Networks and Applications*, vol. 11, no. 5, pp. 711–722, 2006.

[23] J. Ho, D. W. Engels, and S. E. Sarma, "HiQ: a hierarchical Q-learning algorithm to solve the reader collision problem," in *Proceedings of the International Symposium on Applications and the Internet Workshops (SAINT '06)*, pp. 88–91, January 2006.

[24] Z. Zhou, H. Gupta, S. R. Das, and X. Zhu, "Slotted scheduled tag access in multi-reader RFID systems," in *Proceedings of the 15th IEEE International Conference on Network Protocols (ICNP '07)*, pp. 61–70, Beijing, China, October 2007.

[25] T. Dimitriou, "A secure and efficient RFID protocol that could make big brother (partially) obsolete," in *Proceedings of the 4th Annual IEEE International Conference on Pervasive Computing and Communications (PerCom '06)*, pp. 269–274, Pisa, Italy, March 2006.

[26] W. Choi and B.-H. Roh, "Backward channel protection method for RFID security schemes based on tree-walking algorithms," in *Proceedings of International Conference on Computational Science and Its Applications*, pp. 279–287, 2006.

[27] S. A. Weis, S. E. Sarma, R. L. Rivest, and D. W. Engels, "Security and privacy aspects of low-cost radio frequency identification systems," *Security in Pervasive Computing*, vol. 2802, pp. 201–212, 2004.

[28] T. L. Lim, T. Li, and S. L. Yeo, "Randomized bit encoding for stronger backward channel protection in RFID systems," in *Proceedings of the 6th Annual IEEE International Conference on Pervasive Computing and Communications (PerCom '08)*, pp. 40–49, March 2008.

[29] L. Lu, Y. Liu, and X. Y. Li, "Refresh: weak privacy model for RFID systems," in *Proceedings of the 29th Conference on Information Communications (INFOCOM '10)*, March 2010.

[30] RF Code, 2011, http://www.rfcode.com/.